PAPER • OPEN ACCESS

Multispectrum rotational states distribution thermometry: application to the $3v_1 + v_3$ band of carbon dioxide

To cite this article: R Gotti *et al* 2020 *New J. Phys.* **22** 083071

New Journal of Physics
The open access journal at the forefront of physics

Deutsche Physikalische Gesellschaft DPG
IOP Institute of Physics

Published in partnership with: Deutsche Physikalische Gesellschaft and the Institute of Physics

OPEN ACCESS

RECEIVED
16 April 2020

REVISED
16 July 2020

ACCEPTED FOR PUBLICATION
22 July 2020

PUBLISHED
25 August 2020

PAPER

Multispectrum rotational states distribution thermometry: application to the $3\nu_1 + \nu_3$ band of carbon dioxide

R Gotti[1,5], M Lamperti[1], D Gatti[1], S Wójtewicz[1,2], T Puppe[3], Y Mayzlin[3], B Alsaif[4], J Robinson-Tait[3], F Rohde[3], R Wilk[3], P Leisching[3], W G Kaenders[3], P Laporta[1] and M Marangoni[1,5]

[1] Dipartimento di Fisica-Politecnico di Milano and IFN-CNR, Via Gaetano Previati 1/C, 23900 Lecco, Italy
[2] Institute of Physics, Faculty of Physics, Astronomy and Informatics, Nicolaus Copernicus University in Torun, Grudziadzka 5, 87-100 Torun, Poland
[3] TOPTICA Photonics AG, Lochhamer Schlag 19, 82166 Gräfelfing, Germany
[4] Clean Combustion Research Center, King Abdullah University for Science and Technology, Thuwal, Saudi Arabia
[5] Authors to whom any correspondence should be addressed.

E-mail: riccardo.gotti@polimi.it and marco.marangoni@polimi.it

Keywords: primary thermometry, molecular spectroscopy, frequency combs

Abstract

In this paper we propose multispectrum rotational states distribution thermometry as an optical method for primary thermometry. It relies on a global fitting of multiple absorption lines of the same band at different pressures. The approach allows leveraging both the temperature-dependent Doppler width and the temperature-dependent distribution of line intensities across the ro-vibrational band. We provide a proof-of-principle demonstration of the approach on the $3\nu_1 + \nu_3$ band of CO_2, for which several accurate line-strength models of both theoretical and experimental origin are available for the global fitting. Our experimental conditions do not allow to test the methodology beyond a combined uncertainty of 530 ppm, but the comparative analysis between different line-strength models shows promise to reduce the error budget to few tens of ppm. As compared to Doppler-broadening thermometry, the approach is advantageous to mitigate systematic errors induced by a wrong modelling of absorption line-shapes and to reduce, for a given experimental dataset, the statistical uncertainty by a factor of 2. When applied in a reverse way, i.e. using a gas of known temperature, the approach becomes a stringent testbed for the accuracy of the adopted line-strength model.

1. Introduction

The microscopic thermal energy, given by the product of the Boltzmann constant (k_B) with the thermodynamic temperature (T), influences several macroscopic parameters of different physical systems. By measuring those parameters, it is possible to derive k_BT and thus k_B if T is known, or T if the value of k_B is kept fixed. The determination of T starting from k_B has emerged as a compelling goal since the recent redefinition of the kelvin in terms of a fixed value of the Boltzmann constant ($k_B = 1.380\,649 \times 10^{-23}$ J K^{-1} [1]), rather than as a fraction of the temperature of the triple point of water. Therefore, all physical systems governed by equations of state can be exploited as primary thermometers for calibration-free measurements of the thermodynamic temperature, in other words for a direct realization of the new kelvin [2–4]. Examples of primary thermometers are acoustic gas thermometers, which exploit the relation between the thermal energy and the speed of sound in a monoatomic gas [5], dielectric constant gas thermometers, based on the pressure dependence of the electric susceptibility of a monoatomic gas [6], and Johnson noise thermometers, where the temperature is accessed via the electronic noise in electrical conductors [7]. The lowest systematic uncertainties reported so far for these thermometers are at the level of few ppm or even below [8–10].

Among primary thermometry techniques, Doppler broadening thermometry (DBT) gained relevance within the international community because it is an optical method

providing an independent cross-check of other primary approaches. DBT is based on retrieving the Doppler width ($\Delta\nu_D$ full-width at half-maximum) from the highly accurate observation of an atomic or molecular transition of a gas at thermodynamic equilibrium. The well-known physical relation $\Delta\nu_D = \frac{\nu_0}{c}\sqrt{8\ln 2\frac{k_B T}{M}}$, where ν_0 is the line-center frequency, c the speed of light in vacuum and M the atomic or molecular mass, allows for the determination of the thermal energy and thus of the gas temperature T once k_B is fixed to the recommended value. After the proposal by Bordé [11] and the pioneering experimental demonstration on ammonia (NH_3) around 10 μm [12], DBT moved to the near-infrared region, where the linearity of detectors is considerably higher, targeting molecular samples simpler than ammonia, such as carbon dioxide (CO_2) [13] and water (H_2O) [13–15]. These first measurements at very high signal-to-noise ratio on a single isolated line allowed to achieve uncertainties at the 100 ppm level and to identify at the same time the major hurdle for accurate DBT determinations, namely the impact of collisional effects (in particular the speed dependence of the relaxation rates [16–18]) on the absorption line-shape, and the uncertainty deriving from a wrong modelling of it. Even at pressures of few Pascal where the Doppler effect is prevailing, the uncertainty budget was recently found dominated, at the 14 ppm level, by the line-shape model used for the fitting of absorption spectra [19]. This issue was circumvented by measuring the very intense atomic transitions of a Cs vapor at pressures as low as 10^{-5} Pa, but at the price of further sources of systematic errors, at the 70 ppm level, due to the hyperfine structure and the saturation of the transitions [20].

In an effort of overcoming the line-shape bottleneck, optical thermometry methods based on absorbance measurements, rather than Doppler width, have been developed, such as rotational-state distribution thermometry (RDT) [21], line-absorbance analysis [22] and line-strength ratio thermometry (LRT) [23]. RDT is based on the retrieval of the line-center absorbances of as many possible transitions of a given ro-vibrational band and on the fitting of this absorbance distribution to a model function that relates it to the gas temperature. A first demonstration given by a dual-comb spectrometer [21] on the $\nu_1 + \nu_3$ band of $^{12}C_2H_2$ at a single pressure of 60 Pa returned a 4-fold improvement of the statistical error as compared to a DBT analysis, yet at the price of a rather large systematic error of 600 mK due to the simple Gaussian fit applied to each absorption profile. Line-absorbance analysis, instead, focuses on a single line observed at very high signal-to-noise ratio and relies on the fact that at decreasing pressures the ratio between line-center and integrated absorbance tends to a straightforward temperature-dependent limit dictated by the Gaussian line-shape; therefore, extrapolation to zero-pressure of this experimental ratio may return the gas temperature, at least as long as the absorption spectra are fitted properly. By this approach an important 6-fold reduction of the statistical uncertainty was obtained with respect to a DBT analysis, but the systematics due to the line-shape model used to retrieve absorbances still need to be assessed [22]. Finally, LRT is an approach to extract very accurately the gas temperature T as a function of a reference temperature T_R from the precise measurement of the line-strength ratio of two transitions at the two temperatures. Such a ratio approach has the double advantage of making the temperature determination independent of the partition function and only weakly dependent on the line-shape model used to compute absorbances and thus line-strength ratios. Simulations predict for LRT accuracies at the ppm level when applied to optical transitions of carbon monoxide (CO) around 4200 cm^{-1} in the range 80–700 K [23].

In this work we introduce an evolution of RDT that relies on a different temperature-dependence model for the absorbances, on the inclusion of collisional effects in the fitting of experimental spectra and on a global minimization routine over all lines and pressures that strongly reduces the number of fitting parameters and thus their correlations. The target purposely chosen for this new thermometric approach, hereafter referred to as multispectrum rotational states distribution thermometry (MRDT), is the $3\nu_1 + \nu_3$ band of carbon dioxide, for which several highly accurate line-strength models are available, based on both *ab initio* calculations and experimental data [24–28]. Using them as constraints for the multiple fitting procedure has the advantage to mitigate the impact of the line-shape model on the retrieved temperature, yet at the price of a bias given by the selected line-strength model. We provide a first empirical estimate of the accuracy of MRDT by analyzing with different models three independent measurement runs over 32 lines at five different pressures as performed with a cavity-ring-down spectrometer. Due to technical limitations of our setup, we could not verify the global uncertainty of the method beyond 530 ppm, but reported results show a potential to reduce it down to few tens of ppm.

2. The optical thermometer

The thermometer, sketched in figure 1, consists of a broadband highly sensitive and accurate optical spectrometer [29]. The probe source is a continuously tunable laser (CTL model, from Toptica) that exhibits a mode-hop-free tuning range of 100 nm, from 1525 to 1625 nm. To synthesize precise and accurate frequency scans, the CTL is phase locked to an erbium frequency comb (Toptica FFS,

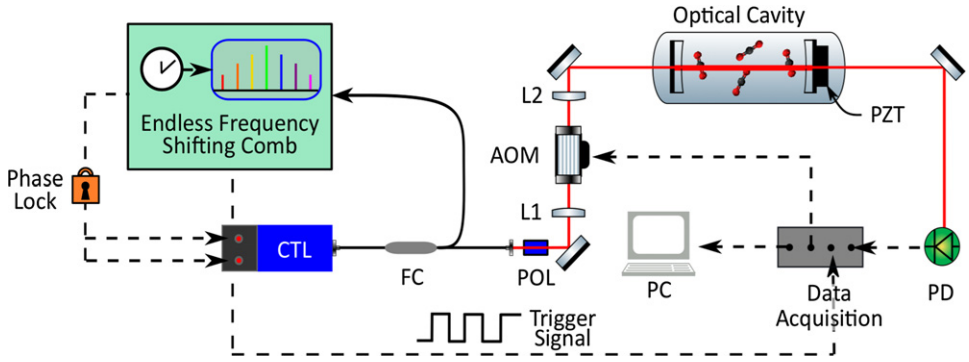

Figure 1. Experimental layout of the spectrometer. CTL: continuously tunable diode laser; FC: fiber coupler; POL: light polarizer; L1, 2: lenses; AOM: acousto-optic modulator; PZT: piezoelectric transducer; PD: photodetector; PC: personal computer. Black solid lines refer to fiber paths, black-dashed lines to electronic connections and red lines to free-space paths.

$f_{rep} = 100$ MHz) whose frequency axis is smoothly and seamlessly shifted within the entire spectral range of the comb through the external phase modulation approach originally proposed by Benkler *et al* [30]. As described in detail in reference [29], this approach has now evolved in an integrated optoelectronic system that offers comb-referred frequency sweeps at speeds up to 1 THz s^{-1} while keeping the optical frequency tracked with an accuracy better than 50 kHz. This laser system is coupled to a 50 cm long optical cavity, with a finesse greater than 10^5, to perform cavity ring-down spectroscopy (CRDS). An acquisition board digitizes both the cavity-ring down transients that occur when the sweeping laser hits a cavity mode and the timing of each injection, which is in turn mapped to optical frequency through the triggering system described in reference [29]. Thanks to a piezo transducer that slowly dithers the cavity mode pattern from scan to scan, optical spectra may be interleaved to achieve a point spacing lower than the cavity free spectral range (295.5 MHz) for the frequency axis. In our typical experimental conditions—namely scanning speed of 0.17 THz s^{-1} over 2.7 THz and 2 μW of power injected in the cavity—the noise level per spectral point resulted in 6×10^{-10} cm^{-1}, mainly limited by the sampling rate of the ring-down transients of 109 kS s^{-1} imposed by the adopted implementation of the technique [29]. To ensure repeatable and accurate thermodynamic conditions, the cavity is enclosed in a massive aluminum shell, whose temperature is actively controlled by thermofoil stripe heaters at around 300.65 K and is kept inside a wooden box with air recirculation. The temperature stability and uniformity are both at the level of 20 mK. A reference Pt100 sensor placed at a distance of about 3 cm from the gas monitors the temperature to have an independent comparison with the temperature extracted from the spectral analysis. Thanks to a previous work on DBT [19] where the gas temperature was spectroscopically measured with a global uncertainty of 14 ppm, we can exclude an offset between gas temperature and sensor temperature beyond 10 mK (33 ppm), which was neglected in the present work due to a sensor calibrated only within 50 mK (160 ppm).

The spectrometer sensitivity enables us to probe the relatively weak $3\nu_1 + \nu_3$ overtone band of CO_2 at low pressures, from 3.5 to 14.5 Pa, with a corresponding average signal-to-noise ratio ranging from 100 to 500. In these conditions the Doppler effect is dominating over the collisional broadening. The high tuning speed reduces the time needed to acquire a spectrum over the entire band to about 10 min, before the insurgence of relevant drifts of the thermodynamic conditions, mainly due to pressure leaking. The choice of the ro-vibrational band is dictated by the availability of several accurate line-strength models that could be implemented and compared to one another for the retrieval of the gas temperature from the absorbance distribution, and also by the relatively large spacing between neighboring lines, which simplifies the fitting. As already remarked elsewhere [16–19] further advantages of CO_2 as a thermometric substance are the absence of a hyperfine structure, the large saturation intensity and the lack of a permanent dipole moment that could enhance the interactions with the walls of the gas container and eventually lead to further line broadening.

3. Temperature model and fitting procedure

The thermometric method leverages the temperature dependence of the line intensities within a given ro-vibrational band according to the equation [31]:

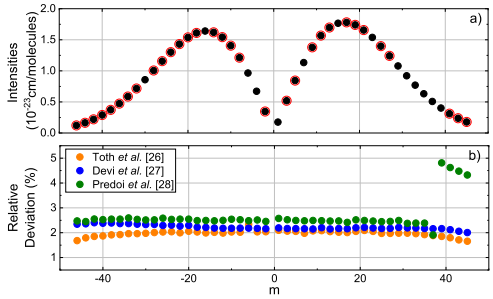

Figure 2. (a) Line intensities $S_m(T_{REF})$ from Zak *et al* [25], which is the reference model for the current version of the HITRAN database. The red circled dots indicate the lines measured in this paper. (b) Normalized relative deviation of the line intensities of the models of Toth *et al* [26] (orange dots), Devi *et al* [27] (blue dots), Predoi *et al* [28] (green dots) with respect to those from Zak *et al* [25].

$$S_m(T) = S_m(T_{\mathrm{REF}}) \frac{Q(T_{\mathrm{REF}})}{Q(T)} \frac{\exp\left(\frac{-E_m''}{k_B T}\right)}{\exp\left(\frac{-E_m''}{k_B T_{\mathrm{REF}}}\right)} \frac{1-\exp\left(\frac{-h\nu_{0m}}{k_B T}\right)}{1-\exp\left(\frac{-h\nu_{0m}}{k_B T_{\mathrm{REF}}}\right)} \quad (1)$$

where $S_m(T)$ is the line-strength of the m-th line at the temperature T to be determined, m is equal to $J''+1$ for R-branch and $-J''$ for P-branch transitions, respectively, $S_m(T_{\mathrm{REF}})$ is the line-strength of the same line at the commonly adopted reference temperature $T_{\mathrm{REF}} = 296$ K, Q is the total internal partition sum, ν_{0m} is the transition frequency of the m-th line while E_m'' is the corresponding lower state energy.

The fitting of the experimental absorption spectra is performed in a global way over all lines and pressures by minimizing the root-mean-square deviation between experimental and fitted absorption, with a line-dependent weight proportional to the average signal-to-noise ratio of the line measurement. Several quantities are kept fixed in the fitting, namely the line-strengths $S_m(T_{\mathrm{REF}})$, as taken by the model (see below), as well as the pressure broadening coefficients and the line-center frequencies, as extracted from HITRAN. Free parameters are the absolute temperature of the gas, which reflects the Doppler width of the lines as well as their intensity distribution across the band, and a dilution coefficient with a linear dependence on time, whose initial value absorbs systematic errors from the line-strength model and from the Q ratio, and its time dependent part takes into account the cavity leakage during the measurement (about 1.1×10^{-3} Torr min^{-1}). There is no fundamental reason why the line-center frequencies and the pressure broadening coefficients are fixed against HITRAN and not left free in the fit, but only a contingent reason, owing to the fact that the SNR of our measurements was not sufficiently high to extrapolate those parameters from the fitting with a precision greater than HITRAN. In this way the fit remains extremely constrained, in a certain sense rigid, but at the same time it takes full advantage of the entire spectroscopic know-how available for the chosen ro-vibrational band. In this respect, the thermometric approach can be viewed as a stringent test for such a spectroscopic knowledge. For the line-shape we adopted a SDVP profile with parameters as specified in the next section.

The use of equation (1) for thermometry implies that errors on all known quantities that appear in the equation contribute to the uncertainty of the retrieved temperature. The line-dependent exponential terms contribute negligibly to the error budget because of the very low uncertainties available for ν_{0m} and E_m''. The partition function ratio at the two temperatures is common mode for all lines and its uncertainty can be neglected introducing a single scale parameter, on the vertical axis of the measurement, in the multiple fitting procedure. The dominant contribution to the error budget comes from $S_m(T_{REF})$ and specifically from the m-dependence of S_m: however, at least for the selected CO_2 band, namely the $3\nu_1 + \nu_3$ band, several independent and recent models are available, both theoretically and experimentally determined, that we consider for possible accurate thermometric measurements. Figure 2(a) shows the line-strength distribution for the model from Zak *et al* [25], which derives from *ab initio* calculations and acts as a reference for HITRAN 2016. Figure 2(b) reports in normalized units the difference between the previous model and those from Toth *et al* [26], Devi *et al* [27] and Predoi *et al* [28] which are inferred from the fitting of experimental spectra. One notices that S_m values may deviate by up to few percent from model to model, but their spectral dependence, which is crucial for the assessment of T, is considerably smaller. The only exception is the discontinuity around $m = 40$ given by the model of Predoi *et al*, which emerges also in their paper [28] yet without a clear explanation. An *a priori* analysis of the error budget for the four models is not feasible, but elements for a quantitative comparative analysis can be obtained by applying them to the same experimental dataset, as it will be shown in the next section.

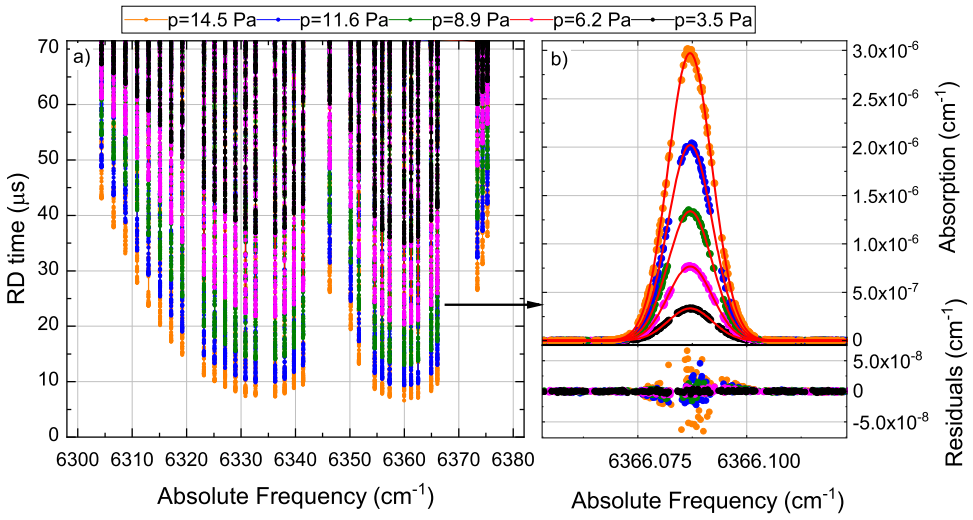

Figure 3. (a) Cavity-ring down measured spectra of the 32 selected transitions of the $3\nu_1 + \nu_3$ band of CO_2 at five different pressures, from 3.5 to 14.5 Pa. Lines that did not match the 6.5 GHz distance criterion discussed in the text are omitted in the figure. (b) Absorption spectrum of the R26 line around 6366 cm^{-1} with corresponding residuals of the fits with a SDVP profile. For the sake of a better visualization of the line the spectral span shown in the figure is about half that considered for the fitting.

4. Experiments and results

As a proof of principle for the thermometric method we performed three independent sets of measurements in the 1567–1587 nm spectral range, covering the P and R branches of the $3\nu_1 + \nu_3$ band of CO_2: each set encompasses five CRDS spectra at different pressures, from 3.5 to 14.5 Pa. The measurement time per spectrum is 10 min. To simplify the fitting and facilitate a comparative analysis with a single-line DBT approach, we selected for the analysis 32 lines, precisely those isolated from neighboring lines by more than 6.5 GHz (including those from other isotopologues, hot bands and impurities), which is the span used to fit each individual line. Figure 3(a) reports the raw data for a multi-pressure spectrum in ring-down time units, whereas figure 3(b) shows an expanded view over almost 2 GHz of the R26 line in absorption units. Each line is composed of about 400 spectral points. The average signal-to-noise ratio is limited to 250 because of a sub-optimal sampling of the ring-down decays, at every 9 μs due to limitations described in reference [29], which very poorly compares with a ring-down time from 72 to 7 μs depending on the line and on the pressure as evidenced in figure 3(a). Conversely, the acquisition time is a strength of the apparatus, with 10 min needed for a complete spectrum at a single pressure.

Figure 4 reports with black symbols the temperatures retrieved from the three independent sets of measurements using the MRDT approach and line-strength data from Zak *et al* [25]. The temperatures differences between different sets are at the level of 30 mK (100 ppm), thus well within the statistical uncertainty of the fit of about 111 mK (365 ppm) reported as error bar in the figure. The analysis of the same datasets with a standard DBT approach returns more scattered temperature values (blue symbols in figure 4), by up to 200 mK, compared to a statistical uncertainty of the fit of about 260 mK. The DBT analysis was performed through a multi-pressure fit of individual lines followed by a weighted average of the retrieved temperatures. In this case the line-strength is left as a free parameter of the fit for each line. As compared to MRDT we found a higher statistical uncertainty and a larger scatter between the retrieved temperatures, by a factor of 2.2 and 6.7, respectively. This is ascribed to the fact that DBT provides temperature through linewidths while MRDT provides temperature through area ratios across the band, the latter being a more robust procedure in the presence of noise on the vertical and horizontal axis of the measurement. Overall, the MRDT analysis over three sets produces a statistical uncertainty of 79 mK, calculated by dividing 111 mK by the square root of the $N - 1 = 2$ effective number of datasets, with a measurement time per dataset of 50 min under suboptimal experimental conditions.

Coming to systematic uncertainties, we may exploit the reading of the Pt100 temperature sensor for a rough assessment. The average MRDT temperature is 300.759(79) K while that from the sensor is 300.620 K with an absolute uncertainty of 50 mK (1σ). We retain the discrepancy of 140 mK as an estimator for the systematic uncertainty (type B error), not being able to quantify an a-priori error budget for the line-strength model. The addition in quadrature of type B (140 mK) and type A (79 mK) errors returns a global uncertainty of 160 mK for this first demonstration of MRDT, thus at the level of 530 ppm. It is worth noting, however, that the discrepancy with the sensor temperature is even higher for the DBT

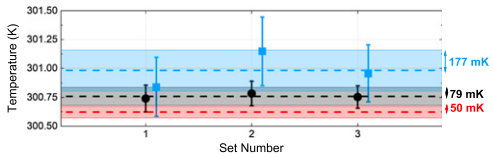

Figure 4. Temperatures retrieved for the three experimental datasets from MRDT (black points) and DBT (blue squares, laterally offset for sake of clarity). Error bars reflect only statistical errors and have been calculated as standard deviations of the individual fits. The shaded areas correspond to the 1-σ confidence interval of the averaged temperatures obtained from MRDT (grey), DBT (light-blue) and Pt100 sensor (red).

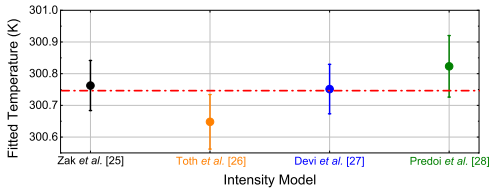

Figure 5. Averaged temperatures retrieved from MRDT using the $S_m(T_{REF})$ values for the selected CO_2 band from Zak *et al* [25] (black dot), Toth *et al* [26] (orange dot), Devi *et al* [27] (blue dot) and Predoi *et al* [28] (green dot). A very good agreement of about 10 mK level (33 ppm) is found when using the two most accurate models from Zak *et al* [25] and Devi *et al* [27]. The red-dashed line corresponds to the mean value (300.746 K) of the four averaged temperatures retrieved applying MRDT with the four previous models.

determination. Actually, these discrepancies are to a high degree due to a weakness of the specific setup used here, which fails to properly quantify the intra-cavity absorption on the more intense lines where the decay time approaches the sampling interval (at every 9 μs). This emerges from the distribution of DBT temperatures, which were anomalously found affected by a line-strength dependence. On the other hand, we could verify that this issue is not due to a wrong choice of the line-shape model, because moving from a Voigt to a speed-dependent Voigt (SDVP with parameters set according to reference [19]), changes the average MRDT and DBT temperatures by 10 and 35 mK respectively. Comparatively, MRDT appears to be more resilient than DBT to errors induced by a change of line-shape modelling due to the comparatively higher weight set by the distribution of line strengths across the band.

To estimate the systematic component due to the choice of a particular line-strength model, we performed MRDT on the same datasets with all models referenced above. For the Predoi model we removed from the fitting the three lines at higher frequency to avoid the bias that occurs at $m > 40$ (see figure 2 and related comment in the text). The averaged temperatures retrieved from the fitting of the three datasets are reported in figure 5, here again with an error bar that only reflects the statistical contribution inferred from the fit. The average deviation from the mean, which is an indicator of the agreement between the models, is 49 mK, which corresponds to a relatively small fractional discrepancy of 160 ppm; interestingly, the mean value (dashed red line in figure 5) is in agreement within only 16 and 5 mK with Zak *et al* [25] and Devi *et al* [27], respectively, which are the models declaring the highest accuracy for the chosen band. Considering the independence and also the different nature of these two models, one theoretical and one experimental, their small discrepancy shows potential to achieve by MRDT a final accuracy much higher than that validated here, at a level of few tens of ppm. This is encouraging for further experimental investigations at higher SNR and in more accurate thermodynamic conditions.

5. Conclusions

We have proposed MRDT as an optical approach to primary thermometry, based on the simultaneous analysis of an ensemble of transitions of the same absorption band at different pressures. MRDT leverages the great progress recently made on the development of highly accurate *ab initio* line-strength models. This is particularly true for carbon dioxide, the thermometric substance adopted here, whose quantitative detection in Earth's atmosphere is crucial for environmental modelling. From an experimental point of view, MRDT requires an optical spectrometer that is capable to capture a large amount of lines in a short time, possibly in an optical cavity to operate at low pressures and simplify the analysis of molecular absorption line-shapes. In this respect, MRDT also leverages recent advancements in broadband molecular spectroscopy, as prompted by the invention of optical frequency combs.

A detailed uncertainty budget for MRDT is not within reach, as we do not have a sufficient knowledge of the theoretical and experimental grounds of the models adopted in the global fitting to reliably infer an uncertainty budget for each of them. This is the reason why we provided a coarse evaluation of the type B error by comparing the MRDT temperature with that from a calibrated Pt100 sensor. The deviation of 140 mK (465 ppm), to some extent due to the calibration uncertainty of the sensor, is likely to be in excess of the effective capability of MRDT. To the end of validating the MRDT accuracy beyond the current level, it will be crucial to adopt in a future gas samples housed in highly accurate temperature environments, for example at the triple point of water or at the melting point of Gallium. Prospectively, to approach the best DBT determinations, the development of line-intensity models with increasing accuracy will be fundamental. The evolution of models over time has been central also for DBT, which benefited from an increasing quality of line-shapes models to move from a global uncertainty of 190 ppm in 2007 [12] to 14 ppm in 2018 [19]. On a different front, MRDT shows potential for fast and accurate temperature measurements in industrial, scientific or metrological domains where high pressures and temperatures are used, and where the fitting of individual lines followed by DBT analysis might be hampered by the presence of multiple overlapping lines.

Acknowledgments

The authors acknowledge a financial contribution from the cooperative project OSR-2019-CCF-1975.34 between Politecnico di Milano and King Abdullah University of Science and Technology and by the project EMPATIA@Lecco ID: 2016-1428. SW is supported by the Polish Ministry of Science and Higher Education program 'Mobility Plus' through Grant No. 1663/MOB/V/2017/0.

ORCID iDs

R Gotti https://orcid.org/0000-0003-3691-814X
M Lamperti https://orcid.org/0000-0001-5972-8723
D Gatti https://orcid.org/0000-0001-9335-821X
M Marangoni https://orcid.org/0000-0002-0522-149X

References

[1] Newell D B *et al* 2018 The CODATA 2017 values of *h*, *e*, *k*, and NA for the revision of the SI *Metrologia* **55** L13
[2] Fischer J *et al* 2018 The Boltzmann project *Metrologia* **55** R1
[3] Pitre L *et al* 2019 Determinations of the Boltzmann constant *C. R. Physique* **20** 129–39
[4] Machin G 2018 The kelvin redefined *Meas. Sci. Technol.* **29** 022001
[5] Moldover M R *et al* 2014 Acoustic gas thermometry *Metrologia* **51** R1
[6] Gaiser C *et al* 2015 Dielectric-constant gas thermometry *Metrologia* **52** S217
[7] Johnson J B 1927 Thermal agitation of electricity in conductors *Nature* **119** 50
[8] Pitre L *et al* 2017 New measurement of the Boltzmann constant *k* by acoustic thermometry of helium-4 gas *Metrologia* **54** 856
[9] Gaiser C *et al* 2017 Final determination of the Boltzmann constant by dielectric-constant gas thermometry *Metrologia* **54** 280
[10] Qu J *et al* 2017 An improved electronic determination of the Boltzmann constant by Johnson noise thermometry *Metrologia* **54** 549
[11] Bordé C J 2005 Base units of the SI, fundamental constants and modern quantum physics *Phil. Trans. R. Soc.* A **363** 2177–201
[12] Daussy C *et al* 2007 Direct determination of the Boltzmann constant by an optical method *Phys. Rev. Lett.* **98** 250801
[13] Castrillo A *et al* 2009 On the determination of the Boltzmann constant by means of precision molecular spectroscopy in the near-infrared *C. R. Physique* **10** 894–906
[14] Moretti L *et al* 2013 Determination of the Boltzmann constant by means of precision measurements of H_2O^{18} line shapes at 1.39 μm *Phys. Rev. Lett.* **111** 060803
[15] Fasci E *et al* 2015 The Boltzmann constant from the H_2O^{18} vibration–rotation spectrum: complementary tests and revised uncertainty budget *Metrologia* **52** S233
[16] Gianfrani L 2016 Linking the thermodynamic temperature to an optical frequency: recent advances in Doppler broadening thermometry *Phil. Trans. R. Soc.* A **374** 20150047
[17] Triki M *et al* 2012 Speed-dependent effects in NH_3 self-broadened spectra: towards the determination of the Boltzmann constant *Phys. Rev.* A **85** 062510
[18] Cygan A *et al* 2010 Influence of the line-shape model on the spectroscopic determination of the Boltzmann constant *Phys. Rev.* A **82** 032515
[19] Gotti R *et al* 2018 Cavity-ring-down Doppler-broadening primary thermometry *Phys. Rev.* A **97** 012512
[20] Truong G-W *et al* 2015 Accurate line-shape spectroscopy and the Boltzmann constant *Nat. Commun.* **6** 8345
[21] Shimizu Y *et al* 2018 Molecular gas thermometry on acetylene using dual-comb spectroscopy: analysis of rotational energy distribution *Appl. Phys.* B **124** 71
[22] Castrillo A *et al* 2019 Optical determination of thermodynamic temperatures from a C_2H_2 line-doublet in the near infrared *Phys. Rev. Appl.* **11** 064060
[23] Amato L S *et al* 2019 Linestrength ratio spectroscopy as a new primary thermometer for redefined Kelvin dissemination *New J. Phys.* **21** 113008

[24] Gordon I E et al 2017 The HITRAN2016 molecular spectroscopic database J. Quant. Spectrosc. Radiat. Transfer 203 3–69
[25] Zak E et al 2016 A room temperature CO_2 line list with ab initio computed intensities J. Quant. Spectrosc. Radiat. Transfer 177 31–42
[26] Toth R A et al 2006 Line strengths of $^{12}C^{16}O_2$: 4550–7000 cm^{-1} J. Mol. Spectrosc. 239 221–42
[27] Devi V M et al 2007 Line mixing and speed dependence in CO_2 at 6348 cm^{-1}: positions, intensities, and air-and self-broadening derived with constrained multispectrum analysis J. Mol. Spectrosc. 242 90–117
[28] Predoi-Cross A et al 2007 Line shape parameters measurement and computations for self-broadened carbon dioxide transitions in the 30012 ← 00001 and 30013 ← 00001 bands, line mixing, and speed dependence J. Mol. Spectrosc. 245 34–51
[29] Gotti R et al 2020 Comb-locked frequency-swept synthesizer for high precision broadband spectroscopy Sci. Rep. 10 2523
[30] Benkler E et al 2013 Endless frequency shifting of optical frequency comb lines Opt. Express 21 5793–802
[31] Rothman L S et al 1998 The HITRAN molecular spectroscopic database and HAWKS (HITRAN atmospheric workstation): 1996 edition J. Quant. Spectrosc. Radiat. Transfer 60 665–710